ORIGINAL PAPER

Effect of propylene glycol on the skin penetration of drugs

Victor Carrer[1] · Cristina Alonso[1] · Mercè Pont[2] · Miriam Zanuy[2] · Mònica Córdoba[2] · Sonia Espinosa[2] · Clara Barba[1] · Marc A. Oliver[1] · Meritxell Martí[1] · Luisa Coderch[1]

Abstract

Propylene glycol (PG) has been used in formulations as a co-solvent and/or to enhance drug permeation through the skin from topical preparations. Two skin in vitro permeation approaches are used to determine the effect of PG on drug penetration. The in vitro Skin-PAMPA was performed using 24 actives applied in aqueous buffer or PG. PG modulates permeability by increasing or diminishing it in the compounds with poor or high permeability, respectively. Percutaneous absorption using pigskin on Franz diffusion cells was performed on seven actives and their commercial formulations. The commercial formulations evaluated tend to have a lower permeability than their corresponding PG solutions but maintain the compound distribution in the different strata: stratum corneum, epidermis and dermis. The results indicate the enhancer properties of PG for all compounds, especially for the hydrophilic ones. Additionally, the Synchrotron-Based Fourier Transform Infrared microspectroscopy technique is applied to study the penetration of PG and the molecular changes that the vehicle may promote in the different skin layers. Results showed an increase of the areas under the curve indicating the higher amount of lipids in the deeper layers and altering the lipidic order of the bilayer structure to a more disordered lipid structure.

Keywords Propylene glycol · Percutaneous absorption · PAMPA · Franz cells · µFTIR

Introduction

Generally, the stratum corneum (SC) is considered the rate-limiting layer of the skin regarding transdermal drug absorption. Drug permeation across the SC depends on the interaction among the skin, drug and other components within the formulation.

Originating from the structure of the SC, two main permeation pathways can be considered: the intercellular route and the intracellular route. In the intracellular route, the chemical is transferred through the keratin-packed corneocytes by partitioning into and out of the cell membrane. This route is not considered the preferred way of dermal diffusion because of the very low permeability through the corneocytes and obligation to partition several times from the more hydrophilic corneocytes into the lipid intercellular layers in the SC and vice versa. The intracellular pathway can gain importance when a penetration enhancer is used, that may modify the corneocyte protein structure and, hence, change their permeability. The intercellular route is the major route of penetration for most compounds, especially when steady-state conditions in the SC are reached. In this

✉ Cristina Alonso
 cristina.alonso@iqac.csic.es

 Mercè Pont
 merce.pont@almirall.com

 Miriam Zanuy
 miriam.zanuy@almirall.com

 Mònica Córdoba
 monica.cordoba@almirall.com

 Sonia Espinosa
 sonia.espinosa@almirall.com

 Clara Barba
 clara.barba@iqac.csic.es

 Marc A. Oliver
 montqt@iqac.csic.es

 Meritxell Martí
 meritxell.marti@iqac.csic.es

 Luisa Coderch
 luisa.coderch@iqac.csic.es

[1] Institute of Advanced Chemistry of Catalonia-CSIC (IQAC-CSIC), Jordi Girona 18-26, 08034 Barcelona, Spain

[2] Almirall R&D Center, Ctra. Laureà Miró 408-410, 08980 Sant Feliu de Llobregat, Barcelona, Spain

case, the chemical is transferred around the corneocytes in the lipid-rich extracellular regions within the SC.

Permeation of a chemical through the SC is basically a diffusion process. For many compounds, the lipophilic SC is the rate-limiting barrier. However, diffusion through the viable epidermis and dermis can be rate limiting when the SC is damaged or affected by disease. Although this pathway is very tortuous and, therefore, much longer in distance than the overall thickness of the SC, the intercellular route is considered to yield much faster absorption due to the high diffusion coefficient of most drugs within the lipid bilayer. Because of the bilayer structure, the intercellular pathway provides hydrophilic and lipophilic regions, allowing more hydrophilic substances to use the hydrophilic and more lipophilic substances to use the lipophilic route. Additionally, it is possible to influence this pathway by certain excipients in the formulation [1].

One long-standing approach to improve transdermal drug delivery uses penetration enhancers (also called sorption promoters or accelerants) that penetrate the skin to reversibly decrease the barrier resistance [2, 3]. One strategy for overcoming the barrier property involves the use of so-called chemical penetration enhancers, which can be combined with skin hydration (occlusion) or increase temperature [4]. PG has been used in skin preparations since 1932 either as a co-solvent for poorly soluble materials and/or to enhance drug permeation through the skin from topical preparations [5, 6] and in different drug delivery systems as in liposomes where PG can modulate biophysical properties of bilayer vesicles [7]. However, the mechanism of action of PG in enhancing drug permeation is not clearly understood [3]. Hoelgaard and Mollgaard [5] suggested a possible "carrier-solvent "effect. Osterenga et al. [8] and Bowstra et al. [9] attributed this effect to dehydratation and Zhang et al. [10] to an increased solubility in intercellular lipids of stratum corneum. Some authors have suggested that PG is not intercalated in the lipid bilayers but may be incorporated into the head group regions of lipids [11]. The interaction of PG with SC has been investigated by many techniques, Differential Scanning calorimetry (DSC), small- and wide-angle X-ray diffraction techniques (SAXS and WAXS) that have proposed the integration of PG into the lipidic hydrophilic regions [12]. Using "in vitro" percutaneous penetration, Trottet et al. [13] found a correlation between the amount of active permeation and amount of PG dosed on the skin. Similar results were obtained using confocal Raman analysis [14, 15]. In the present work, Synchrotron-Based Fourier Transform Infrared microspectroscopy (µFTIR) is presented to add knowledge about the skin enhancer mechanism of PG.

Recently, there has been an exponential increase in the use of the Fourier transform infrared (FTIR) spectroscopic technique in skin science and dermatology. It provides a wealth of information on the cellular and molecular levels of solid and liquid specimens without using external agents such as dyes, stains or radioactive labels [1, 16-19]. µFTIR is a conventional infrared spectrometry technique with little modifications to be adapted to the synchrotron infrared source and microscope. These modifications represent a significant enhancement over conventional IR. Some authors have studied simultaneously the skin composition, structure and molecule penetration [20]. Others have used µFTIR to study the effect of penetration enhancers on the SC lipidic structure and to follow exogenous molecule penetration [21]. Another technique is a rheological analysis that represents an adequate modeling to evaluate the properties of skin to predict the possible modifications due to topical applications and their effects on the skin barrier function [22].

Spectral analysis is a crucial step to draw conclusions from the µFTIR experiments. To extract information from the spectra, many mathematical calculations can be performed e.g. baseline, normalization, second derivative, and principal component analysis. Moreover, when the spectral contribution of a substance is to be determined, other methods arise. In this work, peak fitting and classical least squares (CLS) analyses will be performed. The µFTIR study to determine the effect of PG penetration on the SC lipidic structure will be supported by some in vitro permeability studies of different topical drugs formulated in PG or in aqueous buffer or in their commercial creams.

Predicting human skin permeability of the chemical actives efficiently and accurately is useful to develop dermatological medicines and cosmetics. The evaluation of percutaneous permeation of molecules is one of the main steps in the initial design and later evaluation of dermal or transdermal drug delivery. From the different scientific alternatives to investigate percutaneous absorption phenomena, it is now widely accepted that the diffusion processes of drugs into the skin can be described by Fick's first law [23]. This equation assumes that diffusion occurs in favour of the concentration gradient in other words, from a higher to lower concentration. This principle is applied in recent mathematical models used to describe the dermal absorption through the SC [24]. The permeability constant (K_p) is defined as the steady-state flux of the chemical across the skin (J_{ss}) normalized by the concentration gradient (ΔC_v) and allows comparison of the results for different substances with reasonable accuracy (Eq. 1). Thus, the assessment of the permeability constant (K_p) has been the main focus of permeation models.

$$K_p = \frac{J_{ss}}{\Delta C_v} \tag{1}$$

The Skin-PAMPA is an in vitro assay for skin penetration measurements. The skin-PAMPA membrane was created using cholesterol, free fatty acid and ceramide analogue

compounds that mimic the features of the lipid matrix of the SC [25]. Based on a 96-well plate format, this system allows the screening of compounds and effective prediction of their permeability by calculating the effective permeability coefficients (P_e). The Franz diffusion cell is one of the most widely used systems for in vitro skin permeation studies [26]. Using this methodology, any type or amount of formulation (within the capacity of the donor chamber) may be applied to the skin or to synthetic membranes. The amount of drug that diffuses across the skin or membrane can then be determined. Porcine skin is histologically similar to human skin [27, 28] with a comparable SC thickness of 21–26 µm [29, 30].

In the present work, two skin in vitro permeation approaches are used to determine the effect of PG on drug penetration. Additionally, the µFTIR technique is used not only to study the penetration of the enhancer within the skin but also to study the molecular changes that the vehicle may promote in the different skin layers. Therefore, the effect of vehicles on skin permeation using Skin-PAMPA and Franz diffusion cells with pigskin was determined, and the enhancer effect of PG was considered based on its skin penetration and lipid modification of the skin substrate.

Materials and methodology

Topical actives and formulations

A vast number of topical actives (Table 1) was employed to study the effect of PG in the different permeation models. The actives are indicated in Table 1 and the formulations, self-prepared and commercial ones, are shown in Table 2.

Skin parallel artificial membrane permeability assay (Skin-PAMPA)

In the Skin-PAMPA assay, active permeabilities were studied when they were solved in a solution at the physiological skin surface pH 5.5 (Pion, No. P/N 110151 50 mL) and in PG (Sigma Aldrich, St Louis, MO, USA), at 20 µM. In both cases, a 2% v/v of dimethyl sulfoxide (DMSO) (Sigma-Aldrich, St Louis, MO, USA) was employed.

The Skin-PAMPA sandwiches were purchased from Pion Inc. (Precoated permeability plates; PN 120691). The manufacturer instructions had been followed. Before forming the sandwich, the bottom (donor) plate was filled with 200 µL of the previously described solution (solution at pH 5.5 or PG).

Table 1 Compound (abbreviation), CAS number, manufacturer, MW, log P and type of compound of the selected substances

Compound (abbreviation)	CAS number	Manufacturer	MW	Log P	Type of compound
Azelaic acid (Az)	123-99-9	Sigma	188	− 0.16	Acid
Betamethasone dipropionate (Bet)	5593-20-4	Sigma	505	3.96	Neutral
Bexarotene (Bex)	153559-49-0	Selleck	348	5.50	Acid
Calcipotriol monohydrate (Cal)	147657-22-5	MatTek	413	3.84	Neutral
Clindamycin (Cli)	18323-44-9	Axon Medchem	425	− 1.00	Basic
Clobetasol propionate (Clo)	25122-46-7	AK Scientific	467	4.18	Neutral
Dapsone (Dap)	80-08-0	Fluka	248	1.27	Neutral
Diclofenac sodium (Dic)	15307-79-6	Sigma	296	2.75	Acid
Diphenhydramine (Dip)	58-73-1	Pacific	255	0.52	Basic
Eflornithine (Efl)	70052-12-9	Chem-Impex International	182	4.24	Zwitterion
Finasteride (Fin)	98319-26-7	Fluka	373	− 4.66	Neutral
Fluorouracil (Fo)	51-21-8	Sigma	130	− 0.66	Neutral
Flurandrenolide (Fra)	1524-88-5	Sigma	437	1.56	Neutral
Glycopyrrolate (Gly)	596-51-0	Spectrum Chemical	318	− 0.66	Quaternary salt
Imiquimod (Imi)	99,011-02-6	Ak Scientific	240	− 1.41	Neutral
Ketoconazole (Ket)	65277-42-1	Intex Quimica	531	3.65	Neutral
Lidocaine (Lid)	137-58-6	Sigma	234	0.61	Basic
Metronidazole (Met)	443-48-1	Sigma	171	− 0.46	Neutral
Nicotine (Nic)	22083-74-5	Tocris, UK	162	0.61	Basic
Salicylic acid (Sal)	69-72-7	Sigma	138	− 0.67	Acid
Tacrolimus monohydrate (Tac)	109581-93-3	LC Laboratories	804	5.59	Neutral
Tazarotene (Taz)	118292-40-3	Sigma	351	5.22	Neutral
Terbinafine (Ter)	91161-71-6	Selleck	291	2.36	Basic
Tofacitinib (Tof)	477600-75-2	MedChem Express	312	0.56	Neutral

Table 2 Formulation, concentration (conc.), manufacturer, total recovery and distribution of compounds in pig skin expressed as % of substance for each sample (mean ±SD, $n=6$): surface excess (W), Stratum Corneum (SC), epidermis (E), dermis (D) receptor fluid (RF), dermis and epidermis (D+E) and percutaneous absorption as recovery from E+D+RF (ABS)

	Formulation	Conc	Formulation manufacturer	Abbreviation	Total recovery (%)	W (%)	SC (%)	E (%)	D (%)	RF (%)	D+E (%)	ABS (%)
Bet	Betamethasone dipropionate PG Sol	0.5 mg g⁻¹	Self-prepared	Bet-PG	75.1±17.5	88.4±3.9	5.2±1.9	3.9±1.3	0.6±0.4	2.0±1.4	4.4	6.4
	Diproderm® cream	0.5 mg g⁻¹	MSD	Bet-cre	78.2±23.3	97.3±0.8	1.4±0.8	0.9±0.3	0.4±0.2	0.1±0.1	1.2	1.3
Clo	Clobetasol PG Sol	0.5 mg g⁻¹	Self-prepared	Clo-PG	112.3±8.4	88.1±1.8	5.0±2.8	3.8±1.6	2.4±1.8	0.7±0.4	6.2	6.9
	Clovate® cream	0.5 mg g⁻¹	IFC	Clo-cre	100.3±23.6	95.9±4.6	1.0±1.6	0.9±0.9	1.2±1.8	0.1±0.0	2.0	2.1
Fo	Fluorouracil PG Sol	50 mg g⁻¹	Self-prepared	Fo-PG	77.3±9.1	83.7±3.1	10.4±2.8	4.2±1.8	0.8±0.5	0.9±0.8	5.0	5.9
	Efudix® cream	50 mg g⁻¹	Meda Pharmaceuticals Ltd	Fo-cre	88.2±7.5	97.1±0.1	1.4±1.1	0.6±0.2	0.1±0.1	0.1±0.0	0.7	0.8
Ket	Ketoconazole PG Sol	20 mg g⁻¹	Self-prepared	Ket-PG	89.4±6.4	91.7±2.2	3.3±1.7	3.3±1.2	0.6±0.4	0.5±0.1	4.0	4.5
	Fungarest® crema	20 mg g⁻¹	Janssen, Belgium	Ket-cre	100.7±3.6	94.9±2.3	2.3±2.6	0.6±0.3	0.2±0.1	0.8±0.2	0.8	1.6
Lid	Lidocaine PG Sol	20 mg g⁻¹	Self-prepared	Lid-PG	97.2±9.6	32.4±10.8	4.3±1.1	1.0±0.6	2.3±0.5	60.0±10.6	3.3	63.4
	Dermovagisil® cream	20 mg g⁻¹	Laleham health, UK	Lid-cre	90.7±3.5	90.6±3.8	3.1±0.4	0.3±0.1	0.7±0.2	5.4±3.7	1.0	6.4
Met	Metronidazole	5 mg L⁻¹	Self-prepared	Met-PG	77.1±17.8	37.0±11.0	9.9±1.2	17.0±10.1	5.1±3.2	31.0±19.2	22.1	53.2
	Rozex® gel	7.5 mg L⁻¹	Galderma Laboratories	Met-gel	89.5±7.9	89.0±3.0	1.5±0.3	1.1±0.1	0.4±0.2	8.4±3.0	1.5	9.9
Taz	Tazarotene PG Sol	1 mg g⁻¹	Self-prepared	Taz-PG	75.7±14.2	94.9±1.2	2.5±0.8	1.4±0.9	1.0±0.6	0.3±0.1	2.4	2.7
	Zorac® gel	1 mg g⁻¹	Pierre Fabre Ibérica S.A	Taz-gel	105.7±4.3	97.0±6.5	1.2±0.1	0.5±0	1.2±0.2	0.1±0.0	1.7	1.8

The acceptor plate was filled with 200 μL of fresh Prisma HT Buffer at pH 7.4 and containing 2% v/v DMSO which ensure the sink conditions during the test. The resultant sandwich was incubated for 5 h at room temperature. After the permeation time, the PAMPA sandwich was separated, and 100 μL of both the donor and acceptor compartments was transferred to UPLC plates. The analytical procedure followed for their analysis is detailed as follows. For the effective permeability coefficient (Pe) calculation, the procedure detailed by Ottaviani et al. was followed [31].

Skin preparation for Franz cells and μFTIR

In accordance with an approved Institutional Animal Care and Use Committee protocol, unboiled porcine skin was obtained from the dorsal area (dermatomed skin) of female white/Landrace pigs weighing 30–40 kg. The skin was provided by the Clinic Hospital of Barcelona. Following euthanasia of the pigs, the bristlers were removed carefully with an animal clipper and were subsequently gently washed with water. The hair-clipped skin was dermatomed using a Dermatome GA630 system (Aesculap, Tuttligen, Germany) to a thickness ranging from 500 ± 50 μm, cut into appropriate pieces (2.5 cm inner diameter) and then sealed and stored under vacuum at -20 °C until their use.

Permeation studies using Franz diffusion cells

Static Franz diffusion cells (Lara-Spiral, Courtenon, France) with a nominal surface area of 1.86 cm^2 and a receiver compartment capacity of approximately 3 mL were employed. The OECD Guidelines [32] and published opinions of the Scientific Committee on Cosmetic Products and Non-Food Products [33] were closely adhered to during this study. Additionally, several other classical and updated principles of percutaneous absorption were considered [34].

Unboiled porcine skin was provided from the Department of Cardiology from the Hospital Clínic of Barcelona. Animal handling was approved by the Institutional Review Board and Ethics Committee of Institut d'Investigacions Biomèdiques Agustí Pi i Sunyer. Back skin from Landrace large white pigs weighing 30–40 kg was collected as previously described [35].

The employed skin was thawed and mounted with the top/SC side facing the donor compartment. The receptor chamber was filled with receptor fluid (RF), Dulbecco phosphate-buffered saline at pH 7.4 (Sigma, St. Louis, MO, USA) in MilliQ water with the addition of 0.04% (w/v) gentamicin sulfate salt (Sigma, St Louis, MO, USA) and of 5% bovine serum albumin (Sigma, St Louis, USA). The bovine serum albumin was added following the recommendations of OECD2010 to increase the uptake of lipophilic compounds [36] and maintain sink conditions during all the experiment.

Air bubbles were carefully removed between the skin and RF. The RF was agitated (600 rpm) using a magnetic stirring bar.

The assembled Franz-type cell was placed in a thermostatically controlled water bath maintained at 37 °C and containing a magnetic stirring device, and the skin surface temperature was maintained at approximately 32 °C. To eliminate the damaged skin, the transepidermal water loss value (TEWL) was measured using a Tewameter TM210 system (Courage & Khazaka, Cologne, Germany) at the moment of the formula application, considering correct TEWL values under 15 g m^{-2} h^{-1}. At this point, a finite dose of 10.75 μL cm^{-2} of each formulation was applied to the top of skin delimited by the upper cell. At 24 h, receptor fluid was collected and transferred to a 5 mL volumetric flask and then was stored at − 20 °C until analysis. In the case of skin, the different skin layers were separated as follows. The skin surface was washed with 500 μL of a solution at 0.5% of sodium lauryl ether sulphate (BASF, Ludwigshafen, Germany) followed with 2 × 500 μL of water and wiped with a cotton bud to remove any remaining formulation. Next, 8 strippings were carried out on the surface horny layers of the SC with strips of adhesive tape (D-Square; Cuderm Corporation, Dallas, USA) applied under controlled pressure (80 g cm^{-2} for 5 s). Finally, the viable epidermis (E) was separated from the dermis (D) after heating the skin at 80 °C for several seconds. The wash (W) and cotton bud were extracted into 10 mL of solvent. The stratum corneum (tape strips) (SC) was extracted into 2 mL of extractor solvent. The viable epidermis and dermis were appropriately extracted into 1 mL of extractor solvent. The wash, D-Squame tapes, epidermis and dermis samples were extracted with acetonitrile (Fisher Scientific, UK) containing 0.5% of trifluoroacetic acid (Sigma, USA) (ACN-TFA 0.5%). Thereafter, all the samples were shaken for 30 min and sonicated for 15 min.

Ultra-performance liquid chromatography-tandem mass spectrometry (UPLC-MS/MS)

The wash, D-Squame tapes, epidermis and dermis samples were diluted with water 1:3 (v/v) and filtered (0.45 μm, Millipore) prior analysis by UPLC-MS/MS. The receptor fluid sample levels were determined by UPLC-MS/MS after protein precipitation with ACN-TFA 0.5%, centrifugation at 4000 rpm for 10 min (4 °C) and dilution of the supernatant with water 1:3 (v/v).

The MS detector used was Waters XEVO TQS. The column used was a Waters Acquity UPLCTM BEH C18 (1.7 μm, 2.1 × 50 mm), maintained at 40 °C. The autosampler temperature was 8 °C. The mobile phase A contained 0.05% HCOOH (Sigma, At Louis, MO, USA) plus 2.5 mM of NH$_3$ (Sigma, St. Louis, MO, USA) (pH 3), and the mobile phase B was acetonitrile (ACN). The flow remained stable at 0.400 μL min^{-1} for all compounds. The analytical conditions for the actives are detailed in Table 3.

Imaging of skin cross-sections using Synchrotron-based Fourier transform infrared microspectroscopy (μFTIR)

μFTIR can be used to map skin cryosections. When a sample area is analyzed, many measurements in each map position are performed. Each position means one spectrum. By combining the spatial information with spectral information, 2D images can be created.

μFTIR sample preparation

The same day of slaughter, 10 μL/cm^2 of a substance was applied and gently spread over the skin surface (treated skin section). The incubation of the skin was performed at room temperature (20–25 °C) on a Petri dish with a wet paper filter to avoid drying of the skin. After 30 min of exposure, a biopsy from the treated area covered with aluminum foil to avoid interferences was embedded in CRYO-M-BED (Bright, UK), frozen in nitrogen liquid and stored at − 30 °C. For the preparation of non-treated samples (Blank skin section), a biopsy of skin was taken and then embedded as explained for the PG sample. The day before FTIR analysis, the skin blocks were cut at 6 μm thickness and mounted in a CaF$_2$ window that was 1 mm in thickness and 13 mm in diameter (Crystran, Dorset, UK).

μFTIR experiments

Synchrotron-Based Fourier Transform Infrared microspectroscopy was performed at the MIRAS beamline at the ALBA synchrotron (Cerdanyola del Vallès, Spain) [37]. CaF2 windows containing the cross-sections were placed in a Hyperion 3000 microscope (Bruker, USA) coupled to a Vertex 70 spectrometer (Bruker, USA). The employed detector was a 50 μm HgCdTe (MCT) Detector (10,000–600 cm^{-1}). The infrared spectra were acquired at room temperature in the transmission mode. The data were recorded using an aperture size of 10 μm × 10 μm. The spectra were collected in the 4000–800 cm^{-1} mid-infrared range at a spectral resolution of 4 cm^{-1} with 128 co-added scans per spectrum.

μFTIR data treatment and statistical analysis

To extract spectral information, the OPUS software (Bruker, USA) was used. The obtained data were processed as follows: the spectra with higher intensities than 1.5 a.u. were excluded for the calculations due to the lack of spectral

Table 3 Analytical conditions of the selected substances. Employed abbreviations of UPLC-MS: Cone voltage (CV) in V; Collision energy in eV (EC); Excitation wavelength (λ) in nanometres; Retention time (Tr) in minutes

Compound	Precursor ion (m/z)	Product ion (m/z)	CV (V)	EC (eV)	% Phase A (time)	λ (nm)	Tr (min)
Azelaic acid	187.10	125.0	25	20	85 (i)–55 (1 min)–5 (1.10 min)–85 (1.70 min)	NA*	1.15–1.2
Betamethasone dipropionate	505.25	279.1	20	20	55 (i)–5 (1 min)–55 (1.70 min)	254	1.05
Bexarotene	347.21	186.0	50	–	20 (i)–5 (1 min)–20 (1.70 min)	258	0.99
Calcipotriol monohydrate	395.1	105	15	35	85 (i)–5 (2 min)–85 (2.20 min)	265	1.85
Clindamycin	425.18	126.0	45	25	85 (i)–55 (1 min)–5 (1.10 min)–85 (1.70 min)	200–400	1.04
Clobetasol propionate	467.19	278.0	50	25	20 (i)–5 (1 min)–1.70 (20 min)	246	1.07
Dapsone	249.06	92.0	30	20	85 (i)–60 (1 min)–5 (1.10 min)–85 (1.70 min)	295	1.10
Diclofenac sodium	296.02	215.1	20	20	65 (i)–5 (1 min)–65 (1.70 min)	277	1.08
Diphenhydramine	255.16	167.1	30	20	85 (i)-35 (1 min)–5 (1.10 min)-85 (1.70 min)	220	1.08
Eflornithine	183	120	20	30	5 (i)–95 (3 min)–5 (3.10 min)	NS**	1.82
Finasteride	373.28	57	45	40	65 (i)–20 (1 min)–5 (1.10 min)–65 (1.70 min)	204	1.0
Fluorouracil	129	86	35	15	5 (i)–95 (3 min)–5 (3.20 min)	266	0.4
Flurandrenolide	437.3	361	5	15	62(i)–45 (0.70 min)–5 (1.10 min)–62 (1.20 min)	NS**	0.6
Glycopyrrolate	319.21	116.1	40	25	20 (i)–5 (1 min)–20 (1.70 min)	237	1.14
Imiquimod	241.14	185.1	50	20	85 (i)–55 (1 min)–5 (1.10 min)–85 (1.70 min)	245	1.14
Ketoconazole	531.15	82	40	25	75 (i)–40 (1 min)–5 (1.10 min)-75 (1.70 min)	243	1.07
Lidocaine	235.17	86.1	40	20	95 (i)–60 (1 min)–5 (1.10 min)–95 (1.70 min)	277	1.08
Metronidazole	172	82	40	20	7(i)-24 (0.7 min)-95 (0.8 min)	319	1.05
Nicotine	163	132	30	20	85 (i)–35 (4.10 min)–5 (4.20 min)	260	1.10
Salicylic acid	137	93	45	20	95 (i)–44 (3 min)–10 (3.10 min)–95 (3.20 min)	301	1.86
Tacrolimus monohydrate	804.48	768.0	35	20	45 (i)–5 (1 min)–45 (1.70 min)	200–400	1.23
Tazarotene	352.3	324.1	50	25	71 (i)–88 (0.70 min)–95 (0.80 min)–71 (1.20 min)	NS**	0.60
Terbinafine	292.2	141	30	20	65 (i)–5 (1 min)–65 (1.70 min)	284	0.98
Tofacitinib	313.3	149	45	25	95 (i)–75 (1 min)–5 (1.10 min)–95 (1.70 min)	290	1.21

NA not applicable

NS no signal

quality and presence of saturated regions. Next, each spectrum was manually grouped considering which layer was acquired (epidermis or dermis) and if it was untreated (NT) or treated with PG. The peak positions were determined using OMNIC software version 7.3 (Nicolet, Madison, WI) and a Gaussian–Lorentzian peak fitting after baseline and normalization. Analysis of every spectrum was made, and the average and standard deviations were calculated in every sample. To compare the different spectra groups, principal component analysis (PCA) was performed using the Unscrambler® (CAMO software, Norway) [38].

The spectral analysis is a crucial step to draw conclusions from the µFTIR experiments. To extract information from the spectra, many mathematical calculations could be performed e.g. baseline, normalization, second derivative, and principal component analysis. Moreover, when the spectral contribution of a substance is to be determined, other methods arise. Peak fitting and classical least squares (CLS) analysis have been performed. Peaks and spectral bands are usually studied using the peak fitting method. Experimentally measured bands or peaks are fitted using the theoretical models that create individual peaks from a spectrum that,

when added together, match the original data. Next, the peak parameters, including the amplitude, intensity or the peak position, can be easily determined and subsequently studied in detail. To apply the classical least squares regression (CLS) [39] to the spectral data, the pure compound spectrum of each constituent (loadings) is required. Next, the contribution (scores) of each loading in the dataset can be calculated. These scores are used to create a map showing the distribution of each reference spectrum.

Results and discussion

As shown in Table 1, the selected set of actives comprises a wide chemical diversity, including the following: 1 quaternary salt, 1 zwitterion, 4 acids, 5 bases and 13 neutral compounds. The following results of the different applied methodologies are discussed. Two in vitro skin permeability models have been applied in the present work using synthetic membranes from Skin-PAMPA or pig excised skin mounted in Franz cells.

Permeabilities of topical actives studied using Skin-PAMPA

The actives were all formulated in a buffer solution at pH 5.5 and PG to evaluate by the Skin-PAMPA methodology the permeability of the compound in these solvents. The permeation coefficient (P_e) was calculated using the amounts of activity in each compartment (acceptor and donor) after the diffusion period (5 h), using the procedure detailed by Ottaviani et al. [29]. The P_e provide information about the intrinsic facility of each compound to diffuse across the PAMPA membrane.

The results in both experiments (buffer 5.5 and PG) are compiled in Fig. 1. They showed the high influence of the vehicle on the distribution across the PAMPA membrane. It has to be beard in mind that all actives were evaluated at the same concentration in both solvents to be, permeabilities, easily compared. This means that drug thermodynamic activity was not considered. The different actives could be labelled considering their log P_e: high permeability (log $P_e < -6$), medium permeability (log P_e between -6 and -8) and low permeability (log $P_e > -8$). When the buffer at pH 5.5 was employed, our set of actives showed a high rank of permeability constants (-10 to -5) (solid pattern in Fig. 1). By contrast, when the substances were vehiculized in PG, the permeability constants ranged from -9 to -7 (dotted pattern in Fig. 1). The substances with a high permeability in the buffer solution reduced their permeability when the PG was employed, whereas the opposite effect was observed in the actives with lower permeability constants in the buffer. This effect could be due to the influence of the PG by diminishing the barrier properties of the membrane that may modulate the active permeabilities. PG could modify/solubilize the lipids of the membrane. Then it could diminish its capability to discern the different permeabilities of actives that occurs when applied to the skin. The effect of propylene glycol on the membranes of Skin-PAMPA is currently being studied [40]. Besides, the influence of PG on the skin structure is being deepened in this work using µFTIR.

Based on the Skin-PAMPA permeability representation, compounds of low permeability (log $P_e < -8$) such as Tazarotene and Metronidazole, compounds of medium permeability (log P_e from -6 to -8) such as Fluorouracil, Ketoconazole and Lidocaine and compounds of high permeability (log $P_e > -6$) such as Bethametasone dipropionate and Clobetasol propionate, were chosen to be analyzed by the Franz cell assay both solubilized in PG and formulated in their commercial formulations.
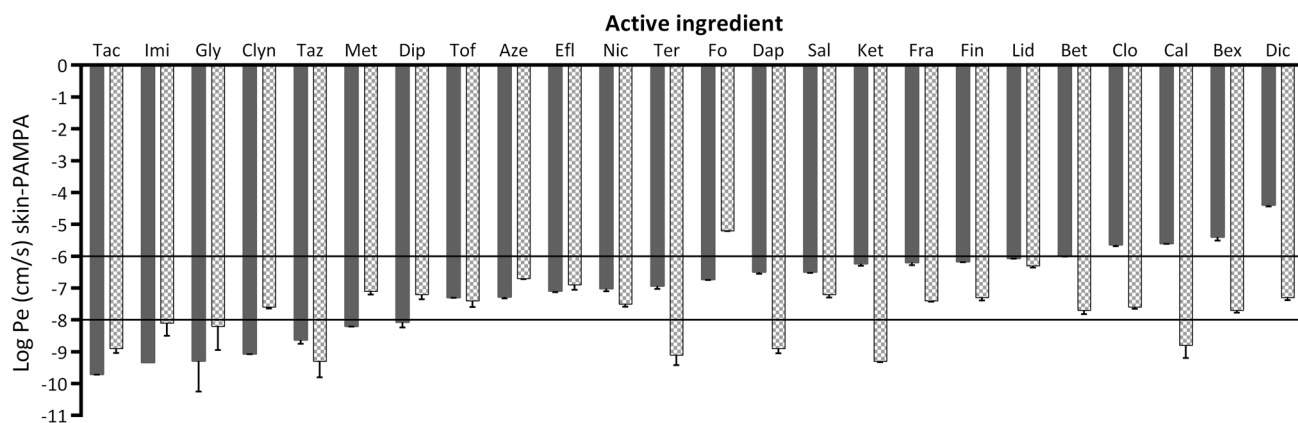
Fig. 1 Skin-PAMPA log P_e (cm s^{-1}) values in buffer solution at pH 5.5 (solid pattern) and in propylene glycol solution (dotted pattern). Actives are classified in high, medium and low permeability and are ordered from lowest to highest log P_e in buffer

Permeabilities of topical actives studied using Franz cells

Franz diffusion cells with dermatomed porcine skin were employed following the corresponding method described in the experimental section for percutaneous absorption determination. The use of Franz diffusion cells allows determination of the actual amount of drug that diffuses across the skin. The distribution in the various skin compartments and receptor fluid, mimicking the systemic compartment of the selected compounds was determined by UPLC-MS/MS. Moreover, the effect of the commercial vehicle comparing the penetration profiles in PG will be discussed. Therefore, this in vitro system has been used to compare the skin penetration profiles of each compound in different formulations, PG solutions, and some of their corresponding commercial formulations (Table 2).

The retention of the actives in the skin was evaluated from the solution of PG, with the objective to keep the formulation as simple as possible, considering in mind that PG is a solvent used in many topical formulations. Moreover, to avoid permeability differences caused by the concentration, the PG solutions were formulated at the same concentration as the corresponding commercial formulation for most of the employed actives. In some cases, however, this implies that different amounts of different actives were applied; moreover, the important drug effect caused by the active saturation degree in each formulation was not considered. It is also important to remark that the receptor fluid was chosen to be the same for all actives, although great differences in lipophilicity exist for all them.

The resulting recovery was acceptable ($100 \pm 25\%$, Table 2) for all the tested formulas. The compounds were recovered from the skin surface (W), stratum corneum (SC), viable epidermis (E), dermis (D) and receptor fluid (RF) (Table 2). The concentrations retained by the SC were not absorbed by the skin and did not contribute to the systemic dose. However, the concentrations found in the E and D could be absorbed and could reach the systemic level [24]. Therefore, the amount of percutaneous absorption (ABS) is normally assumed to be the sum of the concentrations in the E, D and RF. Moreover, for many of the selected actives, their therapeutic effect is done in the E and D receptors are located in the epidermis and the dermis tissue (E + D); thus, the amounts found in such layers are important to know. The amounts of actives in every layer, expressed as a relative percentage of total content, are represented in Table 2 and Fig. 2 for all the actives formulated in PG and in the commercial formulations.

Percutaneous absorption of the 7 evaluated actives in PG and in commercial formulations shows a similar behavior, and the active is distributed following the order W > SC > E > D. The compounds were found to have a reduced distribution when moving in depth through the skin. In both formulations, a maximum percutaneous absorption was found for Lidocaine and Metronidazole followed by clobetasol being tazarotene, the worse absorbed compound. This finding is not completely in accordance with the permeability value from Skin-PAMPA.

It is important to remark that to compare the different formulations it was necessary to evaluate the PG solution with the commercial formulation at the same concentration of active. This means that they were not applied at saturate conditions as it is normally standardized in terms of thermodynamic activity [12, 41]. Then, differences in permeability actives could not have been accurately obtained.
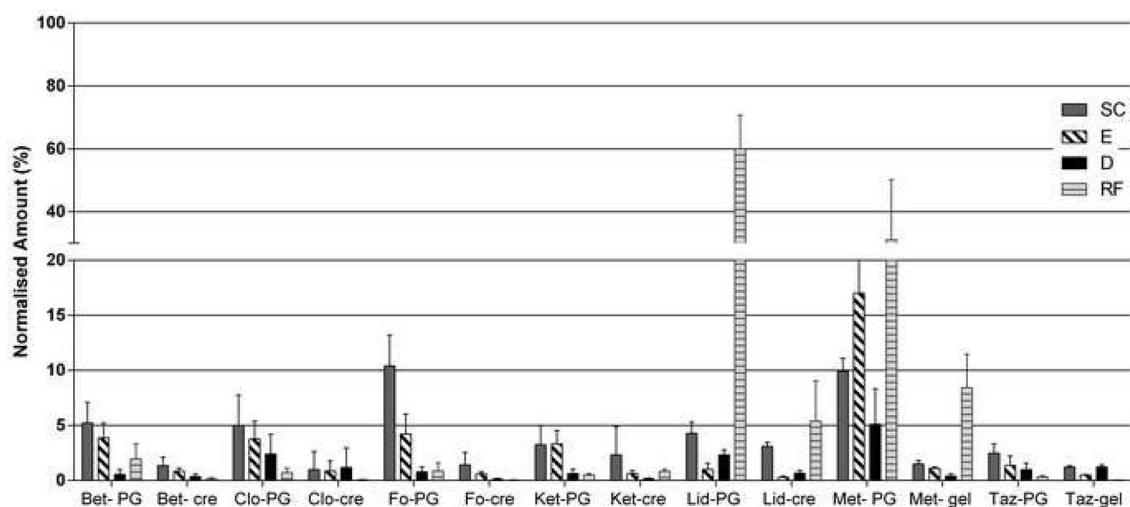
Fig. 2 Cumulative amounts (%) found in the stratum corneum (SC), epidermis (E), dermis (D) and receptor fluid (RF) of Bet, Clo, Fo, Ket, Lid, Met and Taz in PG and their cream or gel commercial formulations (mean $\pm$ SD, $n = 6$)

However, lidocaine and metronidazole presented a different profile than the other compounds. The actives are scarcely retained in the W and SC but are mainly detected in the receptor fluid. Moreover, when the E and D layers are observed, more lidocaine is found in D than in E; however, in all the other PG solutions, the amounts obtained in E are always higher than those in D. Lidocaine and metronidazole are small actives with a relatively low hydrophilic character and quite low melting points, properties that are known to favour skin penetration. Moreover, lidocaine is a basic molecule with a hydrophilic character at pH 5.5 but is lipophilic at pH 7 due to its pKa [42]. The pH gradient at the SC depth and change from hydrophilic property to a lipophilic property of Lidocaine may influence its high diffusion.

The vehicle effect on the compound skin distributions were studied, considering that the PG solutions are formulated at the same concentration as the commercial formulations. A common feature for the PG solutions is that, in every skin layer (SC, E and D), the different actives are much more present than in creams or gels. This leads to the higher absorption observed for PG solutions than creams or gels because the absorbed averages are the sum of E, D and RF. This also occurs for lidocaine and metronidazole, which present a similar pattern when applied in PG than when applied as a cream or gel. However, it should be noted that the lowest penetration of lidocaine and metronidazole in all skin strata occurred in commercial formulations.

Formulation plays a critical role in the delivery of the active into and through the skin. We have been using commercial formulations to see how efficient those formulations to deliver the actives were. In addition, experiments with actives dissolved in PG enabled us to compare permeability in a common solvent. These results, though, need to be taken cautiously since the saturation degree of each active in the vehicle has an impact on the final outcome [3].

It is important to consider the enhancer effect of PG found for all actives studied in front of creams. However, some actives are more sensitive than others to the enhancer. On the one hand, percutaneous absorptions of the most hydrophobic compounds (Bet, Clo, Ket, and Taz) in creams are all approximately 2%, and the effect of PG increases these values to 3–7% (an increase of 200–400%). On the other hand, percutaneous absorption of the most hydrophilic compounds (Fo, Lid and Met) in creams ranges from 1 to 10% and the effect of PG increases these values to 6–60% (Increase of 500–1000%). This indicates that the enhancer effect demonstrated for all compounds is more marked for the hydrophilic compounds, and the possible modification of the skin hydrophobic lipidic barrier facilitates greatly the penetration of the hydrophilic compounds. A different saturated activity of the hydrophilic and lipofilic substances in PG could also be the reason for the changes in permeability of these compounds depending on the formulation. Previous

works with different enhancers also indicate that hydrophilic molecules, owing to their low partition coefficient and high hydrogen bonding potential, would show a dramatic increase in permeation with suitable enhancers. However, lipophilic molecules which move with a relative ease through the SC do not have the same opportunity to act as indicators of enhancement [43-45].

In summary, a compound distribution (W > SC > E > D) was maintained in PG and cream formulations. Moreover, the effect of PG solutions promotes the highest amount of most compounds in all the different layers of the skin (SC, E, D). Additionally, this enhancer effect is more marked for the hydrophilic compounds. The observed enhancer effect of PG in the skin has been widely described [2, 3].

μFTIR study of PG-treated skin

Propylene glycol has been used as a common solvent for many drugs. PG acts by changing the solubility of the compound in the formulation, but it may also act as a fluidizer of the intercellular lipid matrix, acting as a skin enhancer.

Non-treated skin (NT) and skin treated with PG (PG) were analyzed using synchrotron-Based Fourier Transform Infrared microspectroscopy (μFTIR to study the skin alterations when submitted to propylene glycol. Non-dermatomed porcine skin was cross sectioned and analyzed using μFTIR after PG exposure as detailed in the experimental section.

The skin spectrum is displayed in Fig. 3. The two strong absorption bands at approximately 1650 cm^{-1} (amide I) and 1550 cm^{-1} (amide II) are typical protein bands that arise mainly from C–O stretching and N–H bending vibrations, respectively, of amide groups of the peptide backbone in proteins [46]. The absorption bands from 3000 to 2800 cm^{-1} are due to the C–H stretching motions of the alkyl groups present in both proteins and lipids. The signal linked to proteins is a broad band, rather weak compared with the lipids absorption that exhibits four fine peaks at approximately 2850 cm^{-1} (CH$_2$ symmetrical stretching), 2920 cm^{-1} (CH$_2$ asymmetrical stretching), 2870 cm^{-1} (CH$_3$ symmetrical stretching) and 2955 cm^{-1} (CH$_3$ asymmetrical stretching) [47]. A prominent band at 1745 cm^{-1} related to the C-O stretching band of phospholipids, esters and glycerides [48] has also been detected.

The areas under the curve (AUCs) were calculated in the 2800–3000 cm^{-1} and the 1720–1760 cm^{-1} regions in all the spectra to study how lipids are distributed in both cryosections (NT and PG). Combining the AUC values with the spatial information, the 2D images of the AUC distribution were reconstructed (Fig. 3).

Our data show that, for NT and PG, the AUCs are higher in the right part of the images, corresponding to the outermost part of the skin. This agrees with the described higher presence of lipids in the stratum corneum [49]. Comparison
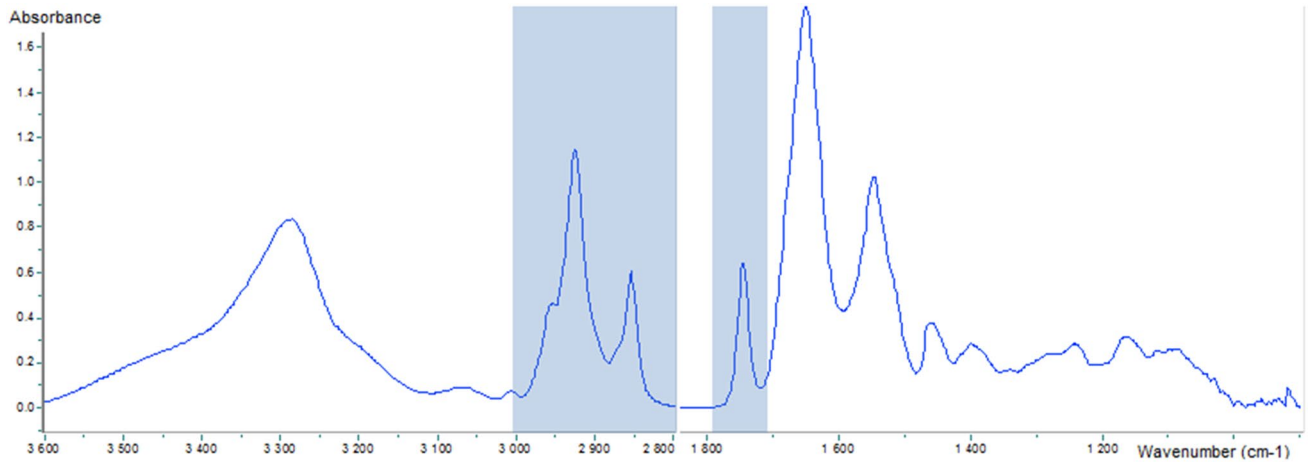
Fig. 3 Baseline FTIR spectrum of skin. The lipidic region (3000–2800 cm^{-1}) and C–O stretching band (1745 cm^{-1}) are shaded

between samples indicates that treatment with propylene glycol in the skin increased the AUCs not only in the outermost region but also in the deeper layers (Fig. 4).

The peak analysed at 1745 cm^{-1} corresponding to C–O stretching of lipids seemed to be predominant after PG treatment in the dermis and epidermis. Not much information

was found about this particular band and the effect that PG may cause. Therefore, further analysis was performed. This dataset was also handled by principal component analysis (PCA) for the epidermis (Fig. 5a) and dermis (Fig. 5b). This technique is commonly used for data classification. It reduces the dimension of the data and extracts only the

Fig. 4 Spatial distribution of area under the curve between (AUC$_{2800–3000}$) and (AUC$_{1780–17,000}$) in non-treated (NT) and treated with propylene glycol (PG) skin cross sections
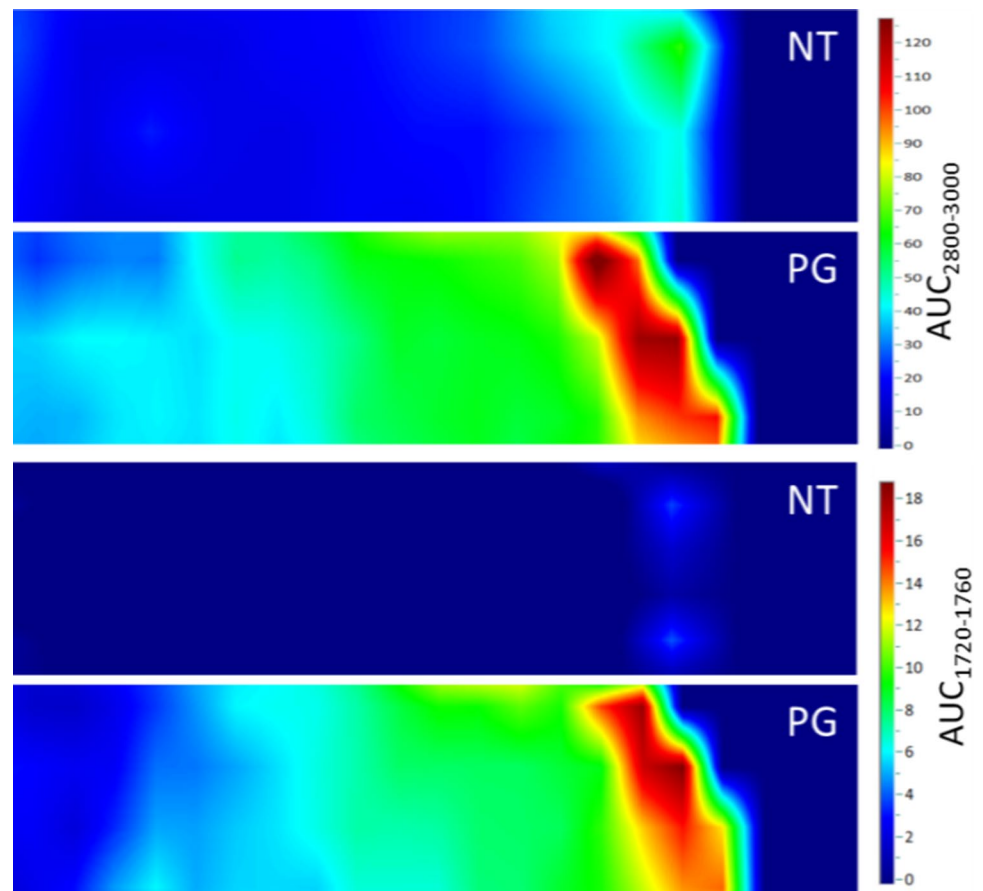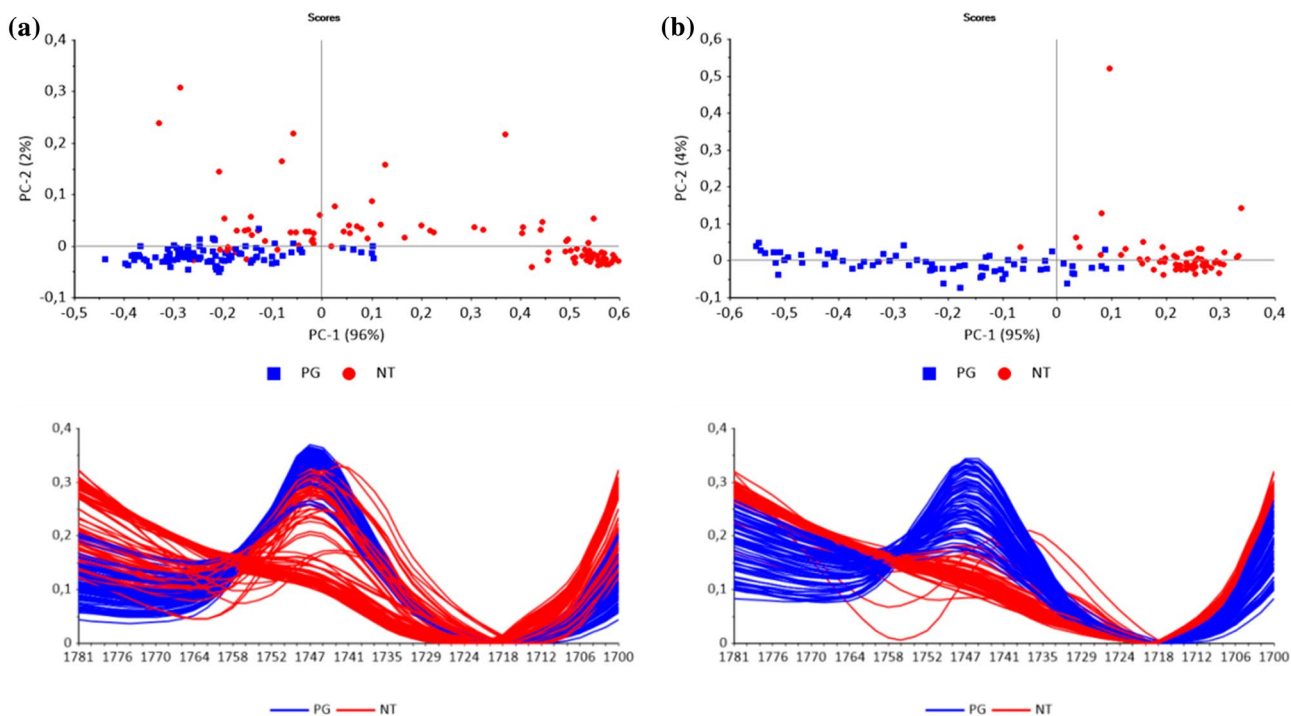
Fig. 5 Principal component analyses of epidermis **a** and dermis **b** at 1745 cm^{-1}. Spectra are colored in red (non-treated) and blue (PG). Upper part contains the representation of PC-1 against PC-2 of all the spectra. The spectra used for the PCA calculation are also displayed in the lower part

relevant information. The resulting principal components (PCs) represent the variance in the data set with decreasing order (PC1 means larger variance than PC2 and so on). The scores represent the original data in the new dimensional space spanned by the PCs. Hence, when plotting PC-1 against PC-2, each spectrum is displayed as a score that carries information about the sample.

In our case, the PC-1 explained more than 95% of the variation of our data in both cases. When representing the PC-1 against the PC-2, in the epidermis and dermis, it could be observed that the treated (blue) and non-treated (red) groups were clearly sorted using the PC-1. This means that, in this region, we can clearly distinguish differences when skin is treated with PG. This fact can also be observed when the spectra of PG and NT samples are displayed together. We could observe that the 1745 cm^{-1} band was more present after propylene glycol treatment and allowed the differentiation of most of the treated or non-treated regions in the epidermis (a) and moreover in the dermis (b) spectra.

Moreover, the position and bandwidth of the lipid stretching bands at 2850 and 2920 are sensitive markers of their chain conformational order: the increased rotational motion of the alkyl chains during the orthorhombic–hexagonal transition and introduction of *gauche* defects in the chains during the hexagonal–liquid transition lead to broadening of the band and its shift to higher wavenumbers [50]. To study the position shifts within our samples, different studies were performed.

The spatial information taken with this µFTIR was used to create images of the position shifts in the NT and PG samples. Thus, the peak fitting method was applied at the 2850 ($\nu_S(CH_2)$) and at 2920 ($\nu_{AS}(CH_2)$) positions for all the spectral data to detect the respective position shifts.

In Fig. 6, the increasing position shift in the 2850 cm^{-1} and 2920 cm^{-1} regions after propylene glycol treatment can be observed. The NT position values fluctuate between 2850 (predominant in the outermost region) until 2855 (in the deeper regions), in accordance with the increasing lipid disorder in the dermis described in other works [50]. When PG is applied the position values are mainly at 2855 and, in some regions, are elevated to 2858. Moreover, after PG treatment no progression of the lipid disorder can be so clearly observed when moving in depth into the skin. Similar information can be extracted regarding the position shift at 2920 in both samples. In the blank, values of 2923 are predominant in the image, and smaller regions with values of 2926 are observed. PG treatment clearly increases the position shift to higher values, with values between 2926 and 2928 predominant in all the mapped area.

To specifically study the position shifts in the SC, E and D, the CLS method was applied. Considering the microscopic image, one spectrum for each skin layer was taken as
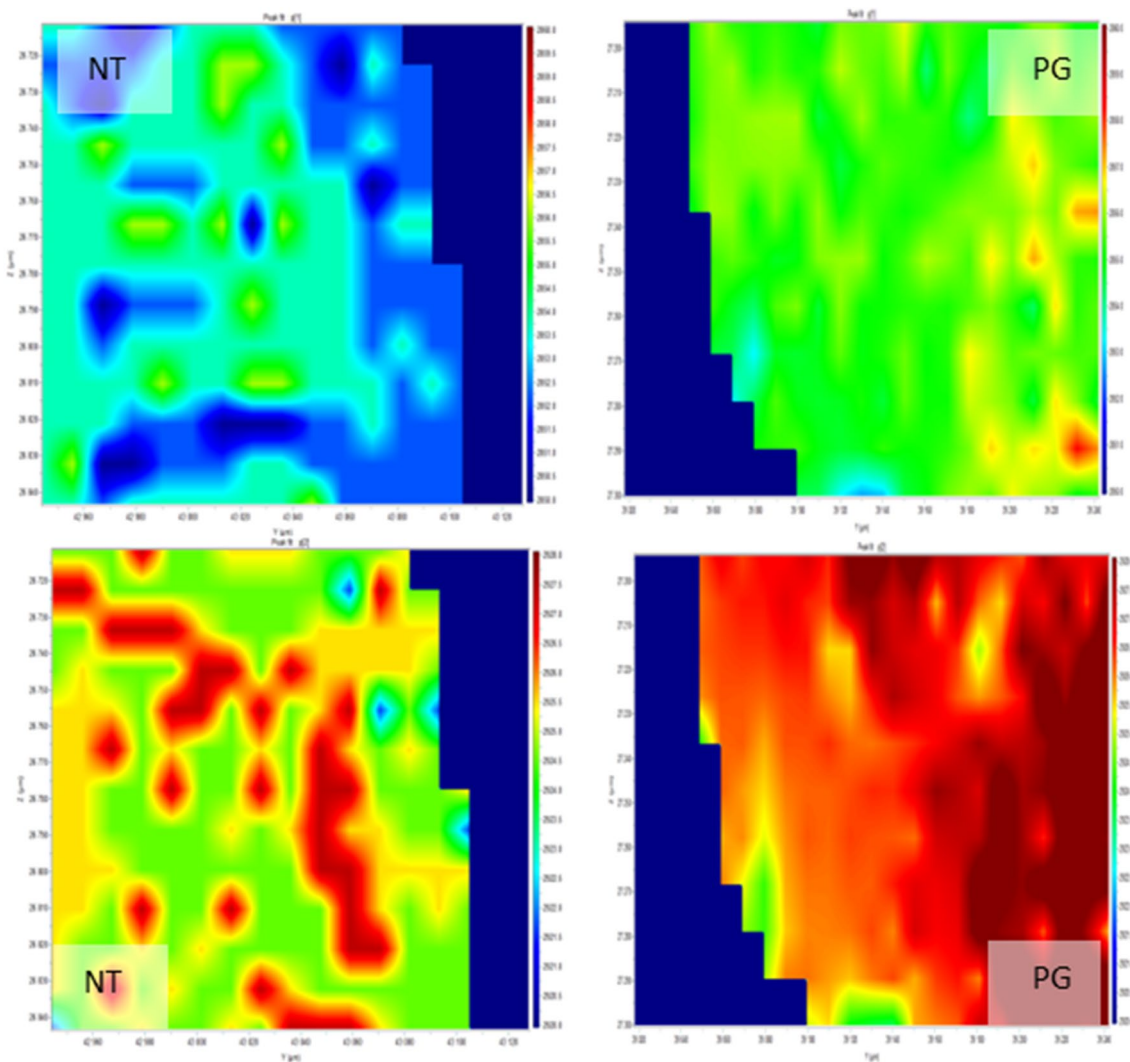
Fig. 6 Upper images contain 2850 cm^{-1} position variations for blank (NT) and PG mapped areas. Lower images contain 2920 cm^{-1} position variation for blank (NT) and PG mapped areas

a reference spectrum and loaded for the CLS score calculations. The obtained scores, with values from 0 to 100, indicate the similarity between each sample spectrum against the three loaded reference spectra. By plotting these scores as an image and overlaying them with the microscopic image, the distribution of each skin layer can be distinguished (Fig. 7).

In green, the stratum corneum is distributed in a narrow area on the outermost part of the skin. The epidermis (in red) indicates a wider region under the stratum corneum. Finally, a small portion of the dermis was recognized in both cases (blank and PG) in the deepest region of the analyzed area. Both samples seemed to present the three layers reasonably distributed if considering the microscopic image.

Hence, considering that the reference spectra were correctly assigned, the loaded reference spectra were analyzed to determine their differences and relate them to the

increased lipid fluidity caused by propylene glycol. The position shifts at 2920 and 2850 for all the 6 spectra: stratum corneum, epidermis and dermis for blank and PG samples, were analyzed using the peak fitting (Fig. 8).

The results confirmed the shifts to higher values after PG treatment. Both positions were sensitive to the PG treatment and were different between the different skin layers. In the three skin layers, comparing PG against Blank, the positions at 2850 and 2920 were increased. Moreover, increasing shifts were observed within each sample when moving more in depth: SC values are lower than those of E and D. Nevertheless, it is important to state that, although the different components were correctly assigned, to have more robustness in our results, more spectra should be studied.

In summary, alteration of the barrier function of propylene glycol includes affecting the bilayer structure of the
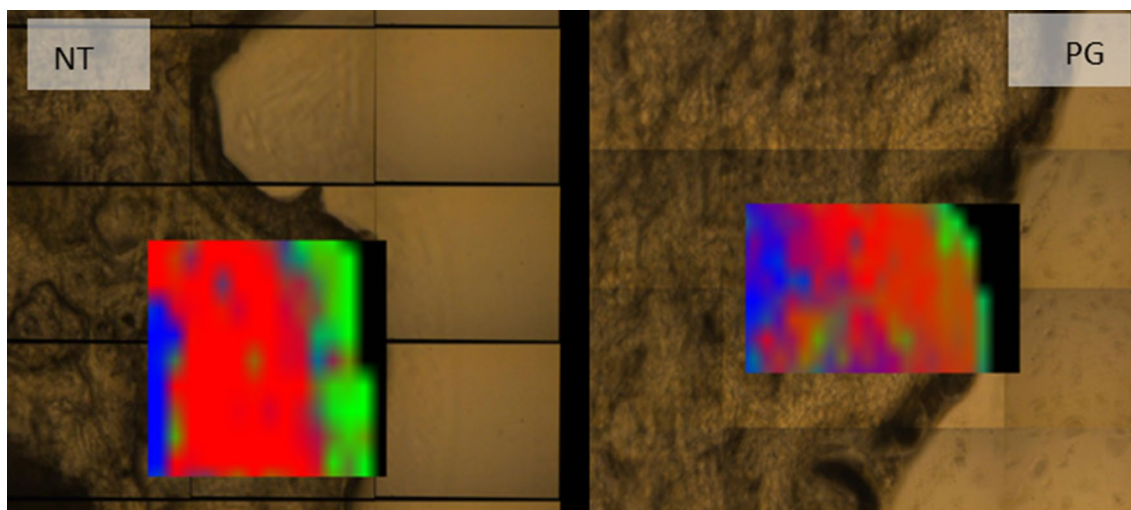
Fig. 7 CLS scores plotted in green (Stratum Corneum), red (epidermis) and blue (dermis) for the non-treated (NT) and propylene glycol treated (PG) samples
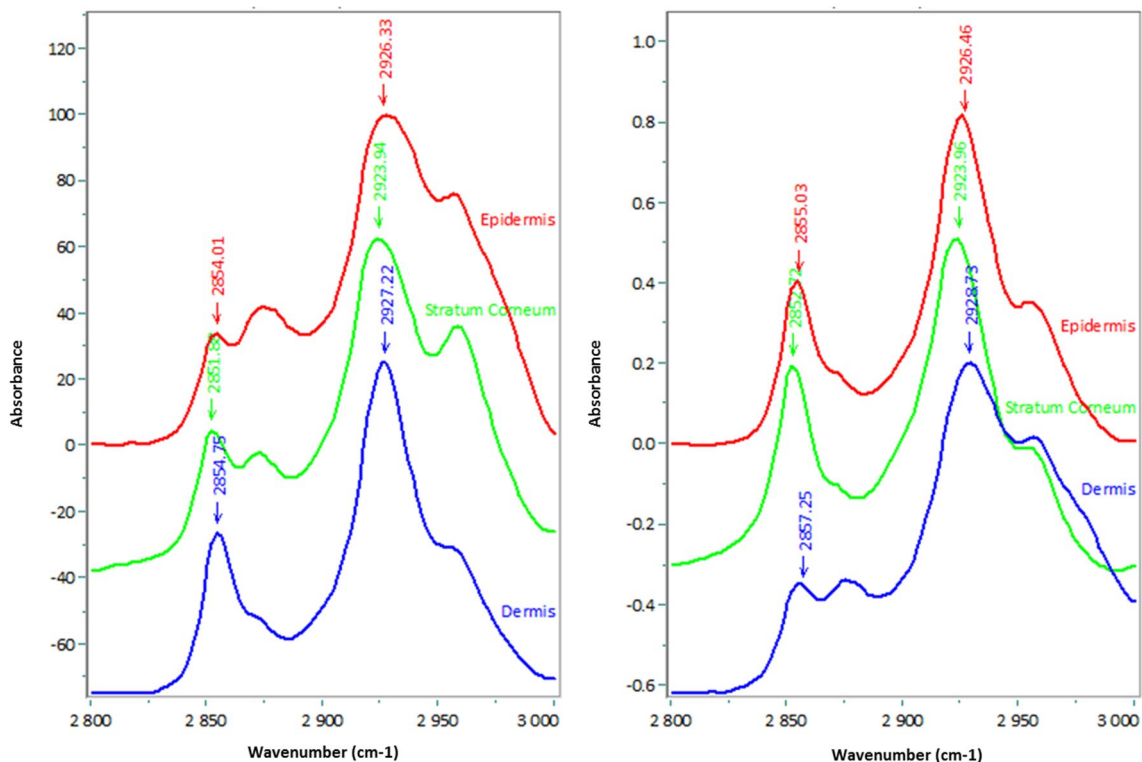
Fig. 8 Classical least squares (CLS) loaded spectra of stratum corneum (green), epidermis (red) and dermis (blue) and the positions at 2850 and 2920 regions

intercellular lipids. Based on numerous experiments [51], the action of solvents such as PG was attributed to a pure cosolvent effect. Maximizing the thermodynamic activity of a drug in the vehicle PG contributes to increased drug uptake into the skin [52]. However, it is unlikely that only one mechanism is responsible for the enhancement of drug penetration, particularly for small molecules. The present study indicates not only an increase in the disorder of lipid in the epidermis and dermis after treatment with propylene glycol but modification of the C-O band attributed to

phospholipids, glycerides and esters in the upper regions of the skin but also in depth.

Conclusions

The in vitro assay Skin-PAMPA with artificial membranes was performed with 24 actives formulated in aqueous buffer at pH 5.5 or PG. When the buffer was employed, the actives showed a high range of permeability constant (from − 10 to − 5), which diminishes (from − 9 to − 7) when the substances are vehiculized in PG. This solvent, which is well-known as a skin enhancer, modulates permeability by increasing the permeability of compounds with poor permeability and diminishing the permeability of actives with high permeability.

Percutaneous absorption with pigskin on Franz diffusion cells was performed on 7 actives with different permeability from the Skin-PAMPA assay, using a pure PG solution and their commercial formulations. The active amounts in the different skin strata (Stratum Corneum, epidermis and dermis) and receptor fluid were determined. In general, the distribution of compounds was found to decrease when moving in depth through the skin. The five creams and 2 gels evaluated tend to have, in all cases, a lower permeability than their corresponding PG solutions, with lower amounts of activity in all the skin layers (SC, E and D), but maintaining the compound distribution in the different strata. The results indicate that the enhancer properties of PG demonstrated for all compounds are more marked for the hydrophilic compounds. The possible modification of the skin lipidic barrier facilitates greatly the penetration of hydrophilic compounds.

The structural skin lipid modification due to PG used on formulations was performed by μFTIR. Treatment of PG in the skin increased the AUCs not only in the outermost region of the stratum corneum but also in the deeper layers indicating the higher amount of lipids in these layers both in the CH_2 and CO vibrational regions of the spectra. Moreover, the epidermis and dermis were found to be modified by altering the lipidic order of the bilayer structure to a more disordered lipid structure. Changes in the C-O band attributed to phospholipids, glycerides and esters could indicate the modification of these compounds. This could be one of the reasons of the poor correlation between permeation methodologies when actives are formulated with PG.

Compliance with ethical standards

Conflict of interest The authors declare that they have no conflict of interest.

Ethical approval All applicable international, national, and/or institutional guidelines for the care and use of animals were followed. Animal handling was approved by the Institutional Review Board and Ethics Committee of Institut d'Investigacions Biomèdiques August Pi i Sunyer (IDIBAPS) Hospital Clínic, Universitat de Barcelona, Barcelona, Spain. The management of the Landrace Large White pigs used in this study conforms to the Guide for the Care and Use of Laboratory Animals published by the United States National Institutes of Health (Eighth Edition. Washington, DC: The National Academies Press, 2011).

Informed consent This study did not require formal informed consent.

References

1. Samaras EG, Riviere JE, Ghafourian T (2012) The effect of formulations and experimental conditions on in vitro human skin permeation—data from updated EDETOX database. Int J Pharm 434:280–291. https://doi.org/10.1016/j.ijpharm.2012.05.012

2. Williams AC, Barry BW (2004) Penetration enhancers. Adv Drug Deliv Rev 56:603–618. https://doi.org/10.1016/j.addr.2003.10.025

3. Lane ME (2013) Skin penetration enhancers. Int J Pharm 447:12–21. https://doi.org/10.1016/j.ijpharm.2013.02.040

4. Prausnitz MR, Langer R (2008) Transdermal drug delivery. Nat Biotechnol 26:1261–1268. https://doi.org/10.1038/nbt.1504

5. Hoelgaard A, Mollgard B (1985) Dermal drug delivery—improvement by choice of vehicle or drug derivative. J Control Release 2:111–120. https://doi.org/10.1016/0168-3659(85)90037-9

6. Nicolazzo JC, Morgan TM, Reed BL, Finnin BC (2005) Synergistic enhancement of testosterone transdermal delivery. J Control Release 103:577–585. https://doi.org/10.1016/j.jconrel.2004.12.007

7. Manca ML, Castangia I, Matricardi P, Lampis S, Fernàndez-Busquets X, Fadda AM, Manconi M (2014) Molecular arrangements and interconnected bilayer formation induced by alcohol or polyalcohol in phospholipid vesicles. Colloids Surf B Biointerfaces 117:360–367. https://doi.org/10.1016/j.colsurfb.2014.03.010

8. Ostrenga J, Steinmetz C, Poulsen B, Yett S (1971) Significance of vehicle composition II. Prediction of optimal vehicle composition. J Pharm Sci 60:1180–1183. https://doi.org/10.1002/jps.2600600813

9. Bowstra JA, Peschier LJC, Brusee J, Boddé HE (1989) Effect of N-alkyl-azocycloheptan-2-ones including azone on the thermal behavior of human stratum corneum. J Pharm 52:47–54. https://doi.org/10.1016/0378-5173(89)90087-2

10. Zhang Q, Li P, Roberts MS (2011) Maximum transepidermal flux for similar size phenolic compounds is enhanced by solvent uptake into the skin. J Control Release 25;154(1):50–7. https://doi.org/10.1016/j.jconrel.2011.04.018

11. Bowstra JA, de Vries MA, Gooris GS, Bras W, Brussee J, Ponec M (1991) Thermodynamic and structural aspects of the skin barrier. J Control Release 15:209–219. https://doi.org/10.1016/0168-3659(91)90112-Q

12. Brinkmann I, Muller-Goymann CC (2005) An attempt to clarify the influence of glycerol, propylene glycol, isopropyl myristate and a combination of propylene glycol and isopropyl myristate on human stratum corneum. Pharmazie 60:215–220

13. Trottet L, Merly C, Mirza M, Hadgraft J, Davis AF (2004) Effect of finite doses of propylene glycol on enhancement of in vitro percutaneous permeation of loperamide hydrochloride. Int J Pharm 274:213–219. https://doi.org/10.1016/j.ijpharm.2004.01.013

14. Pudney PD, Mélot M, Caspers PJ, Van Der Pol A, Puppels GJ (2007) An in vivo confocal Raman study of the delivery of trans retinol to the skin. Appl Spectrosc 61:804–811. https://doi.org/10.1366/000370207781540042

15. Bonnist EY, Gorce JP, MacKay C, Pendlington RU, Pudney PD (2011) Measuring the penetration of a skin sensitizer and its delivery vehicles simultaneously with confocal raman spectroscopy. Skin Pharmacol Physiol 24:274–283. https://doi.org/10.1159/000328729

16. Lademann J, Richter H, Schaefer UF, Blume-Peytavi U, Teichmann A, Otberg N, Sterry W (2006) Hair follicles—a long-term reservoir for drug delivery. Skin Pharmacol Physiol 19:232–236. https://doi.org/10.1159/000093119

17. Alvarez-Román R, Naik A, Kalia YN, Guy RH, Fessi H (2004) Skin penetration and distribution of polymeric nanoparticles. J Control Rel 99:53–62. https://doi.org/10.1016/j.jconrel.2004.06.015

18. Narishetty ST, Panchagnula R (2004) Transdermal delivery system for zidovudine: in vitro, ex vivo and in vivo evaluation. Biopharm Drug Dispos 25:9–20. https://doi.org/10.1002/bdd.381

19. Yu XZ, Jin XP, Yin L, Shen GZ, Lin HF, Wang YL (1994) Influence of in vitro methods, receptor fluids on percutaneous absorption and validation of a novel in vitro method. Biomed Environ Sci 7:248–258

20. Dumas P, Miller L (2003) The use of synchrotron infrared microspectroscopy in biological and biomedical investigations. Vib Spectrosc 32:3–21. https://doi.org/10.1016/S0924-2031(03)00043-2

21. Cotte M, Dumas P, Besnard M, Tchoreloff P, Walter P (2004) Synchrotron FT-IR microscopic study of chemical enhancers in transdermal drug delivery: example of fatty acids. J Control Release 97:269–281. https://doi.org/10.1016/j.jconrel.2004.03.014

22. Manca ML, Matricardi P, Cencetti C, Peris JE, Melis V, Carbone C, Escribano E, Zaru M, Fadda AM, Manconi M (2016) Combination of argan oil and phospholipids for the development of an effective liposome-like formulation able to improve skin hydration and allantoin dermal delivery. Int J Pharm 505:204–211. https://doi.org/10.1016/j.ijpharm.2016.04.008

23. Maibach H (1984) Dermatological formulations: percutaneous absorption. By Brian W. Barry. Marcel Dekker, 270 Madison Avenue, New York, NY 10016. 1983. 479 pp. 16 × 23.5 cm. J Pharm Sci 73: 573–573. https://doi.org/10.1002/jps.2600730442

24. Fitzpatrick D, Corish J, Hayes B (2004) Modelling skin permeability in risk assessment—the future. Chemosphere 55:1309–1314. https://doi.org/10.1016/j.chemosphere.2003.11.051

25. Sinkó B, Kökösi J, Avdeef A, Takács-Novak K (2009) A PAMPA study of the permeability enhancing effect of new ceramide analogues. Chem Biodivers 6:1867–1874. https://doi.org/10.1002/cbdv.200900149

26. Hoang KT (1992) Dermal exposure assessment : principles and applications. U.S. Environmental Protection Agency, Office of Health and Environmental Assessment, Washington, DC, EPA/600/8-91/011B

27. Gray GM, Yardley HJ (1975) Lipid compositions of cells isolated from pig, human, and rat epidermis. J Lipid Res 16:434–440

28. Wester RC, Melendres J, Sedik L, Maibach H, Riviere JE (1998) Percutaneous absorption of salicylic acid, theophylline, 2, 4-dimethylamine, diethyl hexyl phthalic acid, and p-aminobenzoic acid in the isolated perfused porcine skin flap compared to man in vivo. Toxicol Appl Pharmacol 151:159–165. https://doi.org/10.1006/taap.1998.8434

29. Jacobi U, Kaiser M, Toll R, Mangelsdorf S, Audring H, Otberg N, Sterry W, Lademann J (2007) Porcine ear skin: an in vitro model for human skin. Skin Res Technol 13:19–24. https://doi.org/10.1111/j.1600-0846.2006.00179.x

30. Wester RC, Maibach HI (2001) In vivo methods for percutaneous absorption measurements. J Toxicol Cut Ocular Toxicol 20:411–422. https://doi.org/10.1081/CUS-120001866

31. Ottaviani G, Martel S, Carrupt PA (2006) Parallel artificial membrane permeability assay: a new membrane for the fast prediction of passive human skin permeability. J Med Chem 49:3948–3954. https://doi.org/10.1021/jm060230+

32. Guidance document for the conduct of skin absorption studies. OECD Series on Testing and assessment, 2004; No. 28: 1–31, https://doi.org/10.1787/9789264078796-en

33. European Commission the SCCS Notes of Guidance for the Testing of Cosmetic Ingredients (2016) SCCS 1564. 151, https://doi.org/doi:10.2772/47128

34. Schaefer H, Redelmeier TE (1996) Skin barrier: principles of percutaneous absorption. Karger, Basel

35. Carrer V, Alonso C, Oliver MA, Coderch L (2018) In vitro penetration through the skin layers of topically applied glucocorticoids. Drug Test Anal 10:1528–1535. https://doi.org/10.1002/dta.2412

36. Bronaugh RL, Stewart RF, Congdon ER (1982) Methods for in vitro percutaneous absorption studies II. Animal models for human skin. Toxicol Appl Pharmacol 62: 481–488. https://doi.org/10.1016/0041-008X(82)90149-1

37. Benseny-Cases N, Álvarez-Marimon E, Castillo-Michel H, Cotte M, Falcon C, Cladera J (2018) Synchrotron-based Fourier transform infrared microspectroscopy (μFTIR) study on the effect of Alzheimer's Aβ amorphous and fibrillar aggregates on PC12 cells. Anal Chem 90:2772–2779. https://doi.org/10.1021/acs.analchem.7b04818

38. AS, CAMO SOFTWARE. https://www.camo.com/downloads/user-manuals.html. Accessed 20 Nov 2018

39. Vyumvuhore R, Tfayli A, Manfait M, Baillet-Guffroy A (2014) Vibrational spectroscopy coupled to classical least square analysis, a new approach for determination of skin moisturizing agents' mechanisms. Skin Res Technol 20:282–292. https://doi.org/10.1111/srt.12117

40. Alonso C, Carrer V, Espinosa S, Zanuy M, Córdoba M, Vidal B, Domínguez MJ, Godessart N, Coderch L, Pont M (2019) Prediction of the skin permeability of topical drugs using in silico and in vitro models. Eur J Pharm Sci 136:104945. https://doi.org/10.1016/j.ejps.2019.05.023

41. Davis AF, Hadgraft J (1991) Efect of supersaturation on membrane transport: 1. Hydrocortisone acetate. Int J Pharm 76:1–8. https://doi.org/10.1016/0378-5173(91)90337-N

42. Lazar A, Lenkey N, Pesti K, Fodor L, Mike A (2015) Different pH-sensitivity patterns of 30 sodium channel inhibitors suggest chemically different pools along the access pathway. Front Pharmacol 6:210. https://doi.org/10.3389/fphar.2015.00210

43. Jackson M, Mantsch HH (1995) The use and misuse of FTIR spectroscopy in the determination of protein structure. Crit Rev Biochem Mol Biol 30:95–120. https://doi.org/10.3109/10409239509085140

44. Golden GM, Guzek DB, Harris RR, McKie JE, Potts RO (1986) Lipid thermotropic transitions in human stratum corneum. J Invest

Dermatol 86: 255–259. https://doi.org/doi:10.1111/1523-1747.ep12285373

45. Olsztyńska-Janus S, Pietruszka A, Kiełbowicz Z, Czarnecki MA (2018) ATR-IR study of skin components: lipids, proteins and water. Part I: temperature effect. Spectrochim Acta A Mol Biomol Spectrosc 188: 37–49. https://doi.org/doi:10.1016/j.saa.2017.07.001

46. van Smeden J, Bouwstra JA (2016) Stratum corneum lipids: their role for the skin barrier function in healthy subjects and atopic dermatitis patients. In: Agner T (eds), Skin barrier function. Curr Probl Dermatol. Basel, Karger 49:8–26. https://doi.org/10.1159/000441540

47. Rodríguez G, Barbosa-Barros L, Rubio L, Cócera M, Díez A, Estelrich J, Pons R, Caelles J, De la Maza A, López O (2009) Conformational changes in stratum corneum lipids by effect of Bicellar systems. Langmuir 25:10595–10603. https://doi.org/10.1021/la901410h

48. Moghadam SH, Saliaj E, Wettig SD, Dong C, Ivanova MV, Huzi JTL, Foldvari M (2013) Effect of chemical permeation enhancers on stratum corneum barrier lipid organizational structure and interferon alpha permeability. Mol Pharm 10:2248–2260. https://doi.org/10.1021/mp300441c

49. Goodman M, Barry BW (1988) Action of penetration enhancers on human skin as assessed by the permeation of model drugs 5-fluorouracil and estradiol. I. Infinite dose technique. J Invest Dermatol 91:323–327. https://doi.org/10.1111/1523-1747.ep12475655

50. Barry BW, Bennett SL (1987) Effect of penetration enhancers on the permeation of mannitol, hydrocortisone and progesterone through human skin. J Pharm Pharmacol 39:535–546. https://doi.org/10.1111/j.2042-7158.1987.tb03173.x

51. Zhang J, Liu M, Jin H, Deng L, Xing J, Dong A (2010) In vitro enhancement of lactate esters on the percutaneous penetration of drugs with different lipophilicity. AAPS PharmSciTech 11:894–903. https://doi.org/10.1208/s12249-010-9449-1

52. Chen M, Liu X, Fahr A (2011) Skin penetration and deposition of carboxyfluorescein and temoporfin from different lipid vesicular systems. In vitro study with finite and infinite dosage application. Int J Pharm 408:223–234. https://doi.org/10.1016/j.ijpharm.2011.02.006